

Hyperspectral Spectrometry as a Means to Differentiate Uninfested and Infested Winter Wheat by Greenbug (Hemiptera: Aphididae)

MUSTAFA MIRIK,^{1,2} GERALD J. MICHELS, JR.,¹ SABINA KASSYMZHANOVA-MIRIK,¹
NORMAN C. ELLIOTT,³ AND ROXANNE BOWLING⁴

J. Econ. Entomol. 99(5): 1682–1690 (2006)

ABSTRACT Although spectral remote sensing techniques have been used to study many ecological variables and biotic and abiotic stresses to agricultural crops over decades, the potential use of these techniques for greenbug, *Schizaphis graminum* (Rondani) (Hemiptera: Aphididae) infestations and damage to wheat, *Triticum aestivum* L., under field conditions is unknown. Hence, this research was conducted to investigate: 1) the applicability and feasibility of using a portable narrow-banded (hyperspectral) remote sensing instrument to identify and discern differences in spectral reflection patterns (spectral signatures) of winter wheat canopies with and without greenbug damage; and 2) the relationship between miscellaneous spectral vegetation indices and greenbug density in wheat canopies growing in two fields and under greenhouse conditions. Both greenbug and reflectance data were collected from 0.25-, 0.37-, and 1-m² plots in one of the fields, greenhouse, and the other field, respectively. Regardless of the growth conditions, greenbug-damaged wheat canopies had higher reflectance in the visible range and less in the near infrared regions of the spectrum when compared with undamaged canopies. In addition to percentage of reflectance comparison, a large number of spectral vegetation indices drawn from the literature were calculated and correlated with greenbug density. Linear regression analyses revealed high relationships (R^2 ranged from 0.62 to 0.85) between greenbug density and spectral vegetation indices. These results indicate that hyperspectral remotely sensed data with an appropriate pixel size have the potential to portray greenbug density and discriminate its damage to wheat with repeated accuracy and precision.

KEY WORDS greenbug, remote sensing, spectral signatures, vegetation indices, wheat

Greenbug, *Schizaphis graminum* (Rondani) (Hemiptera: Aphididae) is an economically important pest of winter wheat, *Triticum aestivum* L., in the southwestern United States. Greenbugs inject toxic salivary secretions into plant cells, which break down cell walls to facilitate feeding as they extract plant nutrients. Greenbug feeding causes significantly lowered dry weight, leaf area, aerial growth, chlorophyll content, and consequently the photosynthetic rate of barley, *Hordeum vulgare* L.; sorghum, *Sorghum bicolor* L.; and wheat (Castro et al. 1988; Riedell and Blackmer 1999; Nagaraj et al. 2002a,b). Furthermore, severe degenerative changes in vascular cells of susceptible wheat can be caused by greenbug feeding. Morgham et al. (1994) observed that ultrastructural changes include disruption of chloroplast, cellular membranes, and enlargement of the plastoglobuli within the chloroplast. They found cellular organelles degenerated drastically as a result of greenbug feeding to a degree that primary structural features could not be distinguished.

Greenbug feeding manifests as chlorotic and necrotic lesions, leading to the death of infested leaves and eventually the whole plant (Brooks 1991, Riedell and Blackmer 1999). Greenbug infestations in wheat do not occur in any predictable pattern in space and time and usually are not uniform; rather, they occur in clusters referred to “greenbug hot spots” in wheat fields (Yang et al. 2005).

To improve crop production and protection, it is essential to have better tools for detecting stress. Using remote sensing instruments, it is possible to monitor changes in crop health over the course of a growing season (Richardson et al. 2004). The presence of disease or insect feeding on a plant or canopy surface causes changes in pigment and chemical concentrations, cell structure, nutrient and water uptake, and gas exchange, which lead to differences in color and temperature that can modify canopy reflectance characteristics (Raikes and Burpee 1998). Therefore, remote sensing provides a harmless, rapid, and cost-effective means of identifying and quantifying crop stress from differences in the spectral characteristics of canopy surfaces affected by biotic and abiotic stress agents.

In a healthy leaf or canopy, reflectance in the visible (400–700 nm) range is relatively low due to light

¹ Texas A&M University System, Agricultural Research and Extension Center, 6500 Amarillo Blvd. West, Amarillo, TX 79106.

² Corresponding author, e-mail: mmirik@ag.tamu.edu.

³ USDA-ARS, 1301 N. Western Rd., Stillwater, OK 74075.

⁴ West Texas A&M University, Old Main, Ste. 307, Canyon, TX 79016.

absorbed by photosynthetic pigments, particularly in the blue (425–492 nm) and red (645–700 nm) regions of the visible spectrum (Gates et al. 1965). Near infrared (NIR) energy (700–1,900 nm) is reflected by plant cells deep within the leaf, and high internal scattering within leaf tissue is also responsible for higher NIR reflectance compared with other regions of the spectrum (Nilsson 1995). Plant stressors or diseases that cause a reduction in photosynthetic pigment concentrations lead to a reduction in absorption, and, consequently, to an increase in reflectance of light in the visible spectrum. However, reflectance in the NIR wavelengths is decreased as internal leaf structure degenerates. Leaf area decreased by diseases or insect pests also reduces reflectance in the NIR region (Nilsson 1980).

These reflectance differences in the visible and NIR regions have led to the development of spectral vegetation indices. Spectral vegetation indices are mathematical transformations of reflectance values at different parts of the spectrum, intended to normalize the measurements made in varied environmental conditions. Varied environmental conditions may include differences in plant species, solar angle, shading, illumination, canopy coverage, soil background, atmospheric condition, and viewing geometry of device over space and time (Riedell and Blackmer 1999, Yang et al. 2005). In general, some of these indices were designed to measure leaf chemistry, whereas the remaining indices were developed to evaluate the variations in vegetative attributes. Perhaps the best known and most popular indices are the Simple Ratio (SR) proposed by Jordan (1969) and the Normalized Difference Vegetation Index (NDVI) developed by Rouse et al. (1973) by using broad-banded or multispectral remotely sensed data. Since then, these indices have been modified and used under different names, such as the Green Red Ratio (GRR) (Tucker 1979), Soil Adjusted Vegetation Index (SAVI) (Huete 1988), and further derived versions of the SAVI: Transformed SAVI, Modified SAVI, Optimized SAVI, and Generalized SAVI (see Baret and Guyot 1991, Qi et al. 1994, Rondeaux et al. 1996, Gilabert et al. 2002, respectively). With advances in hyperspectral remote sensing instruments, more spectral vegetation indices were developed for detection and quantification of photosynthetic pigments, nutrient deficiencies, and stresses; for example, the Red-Edge Vegetation Stress Index (RVSI) (Merton 1998), Yellowness Index (YI) (Adams et al. 2000), Anthocyanin Reflectance Index (ARI) (Gitelson et al. 2001), and Carotenoid Reflectance Index (CRI) (Gitelson et al. 2002).

Significant correlations between the spectral reflectance data and symptoms of net blotch in barley, glume blotch in winter wheat, and both diseases in spring wheat were reported by Nilsson (1991). Nilsson and Johnsson (1996) reported significant correlations between the radiometric assessment of barley stripe disease and grain yield. Lelong et al. (1998) identified differences in well-developed and stressed wheat canopies by using principal component analysis in an image. Riedell and Blackmer (1999) conducted a

greenhouse study using a portable spectrometer to identify wavebands sensitive to greenbug stress to wheat, and they found that reflectance from the leaf in the 625–635 nm and 680–695 nm as well as the Normalized Total Pigments to Chlorophyll *a* Ratio Index (NPCI) were good indicators of chlorophyll loss and leaf senescence caused by greenbug feeding damage. Yang et al. (2005) used a hand-held radiometer in greenhouse experiments to characterize greenbug stress in wheat and found that a waveband centered at 694 nm and spectral vegetation indices derived from wavelengths centered at 800 and 694 nm were most sensitive to greenbug-damaged wheat.

Although spectral detection and quantification have been successful in plant science, local or widespread occurrence of greenbug infestations and damage to wheat in production fields have not been documented using this technique. A limited number of investigations dealing with remote measurements of crop stress caused by greenbug infestation addressed greenbug damage to wheat growing in controlled environments. However, it has not been confirmed whether the findings of these investigations in greenhouses can be practical in field situations. In a review of a large body of published information, Pinter et al. (2003) concluded that the spectral properties of crop canopies in the field are more complex and not similar to leaves or plants studied under carefully controlled illumination. Therefore, remote sensing research in real-time field use is desirable to provide spatial and temporal information for natural greenbug infestations.

Satellite remote sensing has the limitations of long time intervals between image acquisition and coarse generally spatial resolution. Aircraft remote sensing suffers from difficulty in georeferencing imagery accurately enough to identify subtle, fine scale, changes in greenbug density within the field. These limitations make satellite and airborne remote sensing somewhat problematic for testing the relationship between reflectance and greenbug density. Therefore, a logical first step is to use a field spectrometer for understanding the spectral response of greenbug-stressed wheat canopies and developing spectral signatures because ground-based sensors have better spatial and spectral resolution to differentiate greenbug stress than airborne or space based platforms. In addition, spectral measurements of a greenbug-stressed wheat canopy made with a field spectrometer can be used as a fundamental ground-truth for satellite and aerial images. Little information is available in the literature as to whether remote measurements of reflected spectra from greenbug-infested field-grown wheat can be correlated with greenbug density.

The objective of the current study was twofold: 1) to examine the spectral reflectance throughout the visible and NIR regions of the spectrum of nonstressed wheat canopies and wheat canopies stressed from greenbug feeding; and 2) to investigate relationships between spectral vegetation indices and greenbug density in wheat growing in the field and greenhouse environments by using a hand-held hyperspectral remote sensing instrument. The greenhouse experiment

was conducted to verify how well the results obtained from a controlled environment (greenhouse) correspond to the outcomes of the data collected from fields.

Materials and Methods

Site Locations and Greenhouse Experiment. Naturally occurring greenbug infestations at two locations in Texas were identified in fall 2003 and in spring 2005. The first infestation was in a volunteer winter wheat field in Moore County near Dumas, TX, (35° 84' N, 101° 96' W, altitude \approx 1,098 m) in late fall 2003 (field 1 hereafter). The second infestation was in a winter wheat field in Hardeman County near Chillicothe, TX (34° 25' N latitude, 99° 49' W, altitude \approx 410 m) in early spring 2005 (field 2 hereafter). In addition to natural greenbug infestations in wheat fields, a greenhouse experiment using wheat grown in flats was conducted at the Texas A&M University, Agricultural Experiment Station facilities at Bushland, TX, in spring 2005.

Sampling Procedure. In field 1, eight patches of greenbug-damaged wheat were located in total. Another eight patches of undamaged wheat (neither greenbugs nor visual evidence of greenbug damage were found on wheat) were located as near as possible to the damaged samples through a ground survey on 21 November 2003. In total, eight 0.25-m² sample plots were established in each of the greenbug-damaged and undamaged wheat patches. The plot locations were selected to represent a range of stress severity; thus, sampling was not random. To randomly sample the study field and still have the same range of stress levels would have required many more plots than the logistics of the study could accommodate. Another reason for systematic sampling rather than random sampling is that the greenbug infestations in wheat usually do not occur uniformly but rather in clusters referred to "greenbug hot spots" (Yang et al. 2005), as in field 1. The wheat crop was at approximately vegetative growth stage 30 measured by the Zadok's scale (Zadok et al. 1974). In field 2, two 200-m transects were set up, and 18 1-m² greenbug-damaged wheat plots in total (nine plots for each transect) were established at 20-m intervals on 18 March 2005. To establish control samples, another two 200-m transects were set up in a neighboring uninfested winter wheat field (neither greenbug nor visual evidence of greenbug damage were found on wheat). Eighteen 1-m² undamaged wheat plots were located at 20-m intervals in that field. The wheat variety was the same in field 2 and the neighboring field. The wheat crop was at approximately vegetative growth stage 32 measured by the Zadok's scale in both fields.

The greenhouse experiment involved two treatments: 1) greenbug-infested and 2) uninfested (control) wheat. There were 10 replications of each treatment. On 10 March 2005, 288 wheat seeds with seed spaced at 2.5 by 3.2 cm per flat were planted in each of 20 wooden flats (64 by 61 by 9 cm) containing field soil as the growth medium. Ten randomly selected flats were put in one greenhouse, and the remaining 10

flats were kept in another greenhouse separated by a breezeway. On 2 May 2005 when the wheat was at approximately vegetative growth stage 23, 10 wheat flats were infested with greenbugs at densities of 100 in three flats, 200 in two flats, 500 in three flats, and 700 in the remaining two flats. The remaining 10 flats were kept free of greenbugs. All flats were watered three times per week. Twenty-one days after infesting, flats of both treatments were transported outside of the greenhouse so as to make spectral measurements and take digital images in the full sun.

Remote Sensing Measurements. Spectral measurements were made with an Ocean Optics S2000 hyperspectral hand-held spectrometer (Ocean Optics Inc., Dunedin, FL). The spectrometer is a linear, charge-coupled device-array detector that collects reflectance data from 339.71 to 1,015.52 nm with a continuous spectral resolution \approx 0.33 nm. The dark current and white Spectralon reference readings were taken at the beginning of every eight to 10 samples (approximately every 15 min). The hyperspectral spectrometer was mounted on a pole and elevated \approx 75 cm above the flat surface to collect reflected light from the wheat canopy over 0.37-m² sample areas. The same spectral measurements of the wheat canopy were applied for fields 1 and 2 with the exception of spectrometer elevations above the sample plots. Spectrometer elevations were kept \approx 65 and 220 cm to record the reflectance over 0.25- and 1-m² sample plots for fields 1 and 2, respectively. The field of view of the spectrometer is 25°. To reduce the sheer volume of data recorded for each plot by the spectrometer, adjacent wavelengths were initially averaged to 1-nm intervals. To determine the best band centers and spectral resolutions in relation to greenbug density, the boundaries of the band centers were then increased through nine iterations by averaging every 2, 3, . . . , 10 neighboring bands.

Along with the spectral measurements, high-quality (TIFF) digital images were taken by a Nikon Coolpix5000 digital camera that was mounted on a pole and kept 200 cm above and perpendicular to the flats and sample plots to cover areas slightly larger than the 0.37, 0.25, and 1 m² for greenhouse experiment, and fields 1 and 2, respectively. Before taking digital images in fields 1 and 2, 0.25- and 1-m² frames were placed over the samples, respectively. All images from fields 1 and 2 and greenhouse experiment were subsampled by digitizing the area inside the 0.25- and 1-m² frames and 0.37-m² flats. Both image and reflectance data acquisition started at 1130 and ended at 1330 hours to keep the effect of the sun angle similar for all samples.

Subsampled images were used to determine greenbug damage on leaves caused by greenbug feeding by processing the digital images through ASSESS: Image Analysis Software for Plant Disease Quantification (Lamari 2002). ASSESS measures leaf area, percentage of disease, root length, lesion count, and percentage of soil and vegetative cover (Lamari 2002). The quantitative amount of leaf tissue affected by greenbug was determined by masking and thresholding by using hue saturation intensity (HIS) color space and

Table 1. Greenbug density and damage to winter wheat at two field and one greenhouse location

Study field ^a	Greenbug density (0.37 m ²) and damage (%)	Min.	Mean	Max	SE	LCI (0.95)	UCI (0.95)
Field 1	Greenbug density	123	283	423	33	207	360
	Damage	27	35	43	2	31	40
Field 2	Greenbug density	58	3,183	6,429	522	2,081	4,285
	Damage	7	47	85	5	36	58
GrHs Exp	Greenbug density	15,120	54,209	88,387	7,908	36,320	72,099
	Damage	39	73	98	7	56	89

Min, minimum; Max, maximum; LCI, lower confidence interval; and UCI, upper confidence interval.

^a Field 1, Moore County near Dumas, TX, sampled on 21 November 2003; $n = 8$. Field 2, Hardeman County near Chillicothe, TX, sampled on 18 May 2005; $n = 18$. GrHs Exp, Greenhouse experiment, Texas Agricultural Experiment Station at Bushland, TX, sampled on 23 May 2005; $n = 10$.

saturation values on leaves. The percentage damage by greenbugs was then calculated as lesion pixels/leaf pixels $\times 100\%$.

Aphid Data Collection. In field 1, after reflectance data and image acquisition, an SH 85 Vacuum/Shredder aspirator (Stihl Inc., Virginia Beach, VA) was used to collect greenbugs from the eight sample plots by placing a screen into the hose of the machine and a 0.25-m² heavy metal frame on the ground. The collected greenbugs were gently placed in plastic bags with wheat leaves to keep them alive, and transported to the laboratory. Within 24 h of sampling, greenbugs were counted in the laboratory. In field 2 and the greenhouse experiment, 20 tillers were randomly taken inside of each 1-m² frame and 0.37-m² flat, respectively, and greenbugs were counted on them. Subsequent to counting greenbugs on the 20 tillers, the number of wheat tillers within each frame and flat were tallied, and greenbug densities were estimated as follows: total aphid per frame or flat = (total tillers \times total aphid on 20 tillers) / 20. Greenbug densities were reestimated for fields 1 and 2 and reported in the same unit area (0.37 m²) used in the greenhouse experiment.

Spectral Vegetation Index Computations. A large number of spectral vegetation indices compiled from the literature were calculated to investigate their relationships with greenbug densities. Two of them that had the strongest relationships with greenbug density were chosen for each data set and compared across the fields and the greenhouse experiment. Along with the two indices chosen for each field and the greenhouse experiment, a modified (Peñuelas et al. 1995) Structure Insensitive Pigment Index (SIPI) using different waveband combinations was calculated. The original formulation of this index is as follows:

$$\text{SIPI} = (\rho_{800} - \rho_{445}) / (\rho_{800} - \rho_{680})$$

where ρ_{800} , ρ_{445} , and ρ_{680} are reflectance values from the bands centers at 800, 445, and 680 nm, respectively. The adjusted version of these indices in the present research (Aphid Index; [AI] hereafter) is as follows:

$$\text{AI} = (\rho_1 - \rho_2) / (\rho_3 - \rho_4)$$

where ρ_1 is reflectance in the range from 700 to 850 nm, ρ_2 is from 850 to 950 nm, ρ_3 is from 500 to 750 nm, and ρ_4 is from 500 to 750 nm but greater than ρ_3 . Specifically, (AI) = $(\rho_{761} - \rho_{908}) / (\rho_{712} - \rho_{719})$ was

used in the current study. Throughout this research, the band centers used to calculate spectral vegetation indices were slightly increased or decreased by replacement of modified wavebands for the Ocean Optics hyperspectral data.

S-PLUS 7.0 for Windows (Insightful Inc., Seattle, WA) was used for linear regression analyses to quantify the relationship between vegetation indices and greenbug density. Greenbug density was set as the independent variable and the spectral vegetation indices set as the dependent variable. A paired t -test procedure for comparing greenbug-damaged and undamaged wheat canopies for each field was conducted using S-PLUS 7.0 for Windows.

Results

Greenbug density varied widely between the field and greenhouse experiments (Table 1). The lowest greenbug density with a mean (\pm SE) 283 ± 33 greenbugs per 0.37 m² was found in field 1, whereas the greenhouse experiment had the highest greenbug density with an average $54,209 \pm 7,908$ greenbugs per 0.37 m² (Table 1). Greenbug density in field 2 fell between that of field 1 and the greenhouse experiment with an average $3,183 \pm 522$ greenbugs per 0.37 m² (Table 1). The percentage of damage to wheat due to greenbug feeding ranged from slight (7%) to severe (98%) across the field and greenhouse experiments. Estimated percentage of damage using ASSESS for the study fields and greenhouse experiment are given in Table 1. The highest mean percentage of damage was found in the greenhouse experiment (73 ± 7), whereas field 1 had the lowest average percentage of damage (35 ± 2).

Paired t -test comparisons of undamaged and greenbug-infested wheat canopies yielded significant differences ($\alpha = 0.01$) in all areas of the spectrum examined (Table 2). Representative average reflectance spectra measured from the greenbug-damaged and undamaged wheat canopies are presented in Fig. 1. Figure 1 shows that the spectral characteristics of the wheat canopies were markedly affected by greenbug damage. Regardless of the growth conditions, the reflectance of wheat canopies in the NIR region was significantly lower in contrast to a significant increase in the visible spectrum due to greenbug feeding (Table 2; Fig. 1). The undamaged wheat canopies always

Table 2. Paired *t*-test comparison of percentage of reflectance between greenbug-infested and uninfested winter wheat for two field and one greenhouse experiments at five wavelength intervals

Study field ^a			Wavelength (nm)				
			400–499	400–724	500–599	600–724	725–900
Field 1	Infested vs. uninfested	<i>t</i>	6.88	8.91	11.14	14.81	–18.13
		<i>P</i>	<0.00	<0.00	<0.00	<0.00	<0.00
Field 2	Infested vs. uninfested	<i>t</i>	14.16	10.69	12.72	10.19	–29.83
		<i>P</i>	<0.00	<0.00	<0.00	<0.00	<0.00
GrHs Exp	Infested vs. uninfested	<i>t</i>	3.39	6.07	4.96	7.10	–26.64
		<i>P</i>	<0.00	<0.00	<0.00	<0.00	<0.00

^a Field 1, Moore County near Dumas, TX, sampled on 21 November 2003; *n* = 8. Field 2, Hardeman County near Chillicothe, TX, sampled on 18 May 2005; *n* = 18. GrHs exp, greenhouse experiment, Texas Agricultural Experiment Station at Bushland, TX, sampled on 23 May 2005; *n* = 10.

captured more (reflected less) light than the greenbug-damaged wheat canopies in the range from 400 nm to the red edge shoulder at 720 nm for the greenhouse experiment, 730 nm for field 2, and 740 nm for field 1.

Using the reflectance at certain waveband centers in spectral vegetation indices indicated that there existed very weak to strong associations between the spectral vegetation indices and greenbug data (Table 3). Wavelengths ranging from the green to lower infrared (500–915 nm) were found to be the most informative in terms of exhibiting a good relationship to greenbug density. The best correlations were revealed between greenbug density and ratio-based spectral vegetation indices, particularly NDVI, SR, and their counterparts using different waveband combinations with a spectral resolution of 7 nm. In Table 3, coeffi-

cients of determination for the newly derived AI, and six spectral vegetation indices with the highest *R*² for each of the three data sets (fields 1 and 2 and the greenhouse experiment) are presented. For field 1, AI had the highest relationship with greenbug density (*R*² = 0.69) followed by the Physiological Reflectance Index (PRI; *R*² = 0.45) of Peñuelas et al. (1994) and the Red Green Ratio (RGR; *R*² = 0.17) of Gamon and Surfus (1999). For field 2, AI also had the highest coefficient of determination (*R*² = 0.62), followed by the Infrared Red Ratio (IRR; *R*² = 0.60) of Tucker (1979) and Modified Chlorophyll Absorption Reflectance Index (MCARI; *R*² = 0.55) of Daughtry et al. (2000). In the greenhouse experiment, the highest *R*² values were found for the Green Normalized Difference Vegetation Index (GNDVI) developed by Gitelson and Merzlyak (1997) and NDVI (Rouse et al.

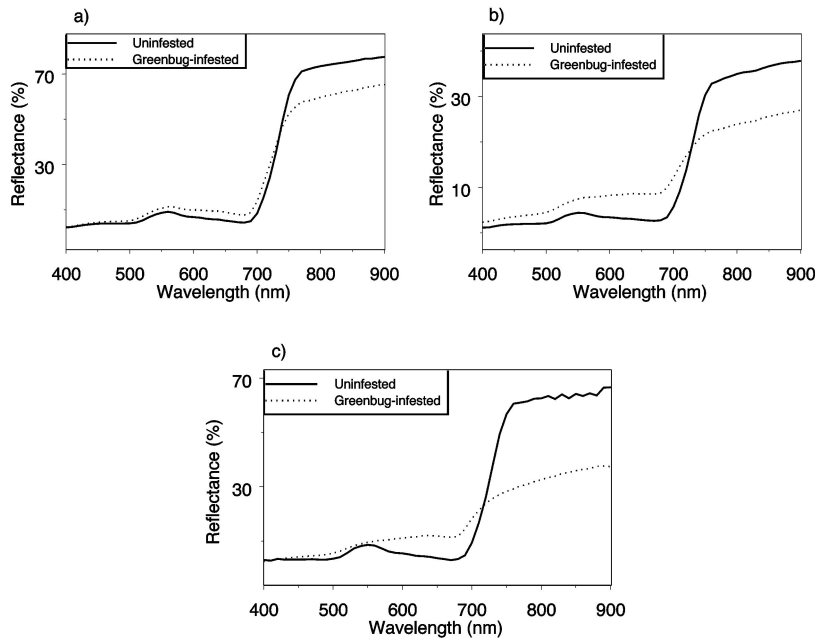


Fig. 1. Percentage of spectral reflectance (400–900-nm range) of greenbug-infested and uninfested winter wheat canopies associated with two field and one greenhouse experiment. (a) Field 1, Moore County, near Dumas, TX; *n* = 8. (b) Field 2, Hardeman County near Chillicothe, TX; *n* = 18. (c) Greenhouse experiment at the Texas Agricultural Experiment Station facilities at Bushland, TX; *n* = 10.

Table 3. Coefficients of determination (R^2) and probability associated with seven spectral vegetation indices and greenbug density on winter wheat for two field and one greenhouse experiment

Index ^a	Field 1 ^b		Field 2 ^b		GrHs Exp ^b		Reference
	R^2	P	R^2	P	R^2	P	
AI	0.69	<0.05	0.62	<0.05	0.59	<0.05	This study
PRI	0.45	0.08	0.20	0.06	0.51	<0.05	Peñuelas et al. (1994)
RGR	0.17	0.31	0.00	0.87	0.36	0.06	Gamon and Surfus (1999)
IRR	0.08	0.51	0.60	<0.05	0.75	<0.05	Tucker (1979)
MCARI	0.09	0.48	0.55	<0.05	0.78	<0.05	Daughtry et al. (2000)
GNDVI	0.01	0.79	0.37	<0.05	0.85	<0.05	Gitelson and Merzlyak (1997)
NDVI	0.07	0.54	0.33	0.05	0.84	<0.05	Rouse et al. (1973)

^a AI = $(\rho_{761} - \rho_{908}) / (\rho_{712} - \rho_{719}) \cdot \rho_{761}$ and ρ_{908} ; reflectance values from wavebands centered at 761 and 908 nm with a spectral resolution = 7 nm. PRI = $(\rho_{550} - \rho_{530}) / (\rho_{550} + \rho_{530})$. RGR = ρ_{600} / ρ_{502} . IRR = ρ_{789} / ρ_{663} . MCARI = $(\rho_{698} - \rho_{670}) - 0.2 \times (\rho_{698} - \rho_{550}) \times (\rho_{698} / \rho_{550})$. GNDVI = $(\rho_{747} - \rho_{537}) / (\rho_{747} + \rho_{537})$. NDVI = $(\rho_{789} - \rho_{649}) / (\rho_{789} + \rho_{649})$.

^b Field 1, Moore County near Dumas, TX, sampled on 21 November 2003, $n = 8$. Field 2, Hardeman County near Chillicothe, TX, sampled on 18 May 2005; $n = 18$. GrHs exp, greenhouse experiment, Texas Agricultural Experiment Station at Bushland, TX, sampled on 23 May 2005; $n = 10$.

1973) were 0.85 and 0.84, respectively. AI ranked fifth with an R^2 of 0.59. The top-ranking indices for each experiment had significant R^2 values ($\alpha = 0.05$) except RGR (Table 3), which had a very low R^2 value even though it ranked third. Although the coefficient of determination for AI ranked fifth among the seven vegetation indices in the greenhouse experiment, this index had consistent, and significant relationships with greenbug density across the three data sets, with the highest associations for fields 1 and 2 (Table 3). It is interesting to note that although R^2 values for AI were not the highest, or even in the top three, in the greenhouse experiment AI had the most consistent results across all three experiments. AI and RGR had positive relationships with greenbug abundance, whereas the remaining exhibited negative associations. The value of an index decreased with increasing damage severity, indicating a negative relationship.

Discussion

A significant increase in the reflectance from the greenbug-damaged canopies in the visible region (400–700 nm) was clear evidence that greenbug feeding reduced the photosynthetic pigment concentrations in particular chlorophylls, which leads to lowered photosynthetic rate of wheat (Castro and Rumi 1987; Riedell and Blackmer 1999; Nagaraj et al. 2002a,b). The reflectance peak from the undamaged wheat at around 550–560 nm occurred due to green light (500–600 nm) being reflected by the green leaf pigments (Riedell and Blackmer 1999). The trend of lower reflectance from the undamaged wheat canopies switched in the red edge spectrum (720–740 nm). From around 730 nm to 900 nm, the greenbug-damaged wheat canopies had lower reflectance than undamaged wheat. This was most likely due to degenerated internal leaf structure, reduced leaf area, and stunting plants caused by greenbug feeding (Castro and Rumi 1987, Castro et al. 1988, Morgham et al. 1994). Spectral responses of field bean leaf infected by *Botrytis fabae* (Malthus and Madeira 1993) and winter wheat infested by greenbug (Riedell and Blackmer 1999) showed similar patterns in reflectance shift.

Botrytis-infected leaf reflectance was higher in the visible and lower in the NIR spectrum than uninfected leaves, which was very similar to the spectral properties of greenbug-damaged wheat leaves (Riedell and Blackmer 1999) and canopies found in this study. However, switches in reflectance from lower to higher when comparing undamaged leaves with damaged leaves occurred around 700 nm in those studies rather than in the range 720–740 nm observed in the current study. These differences may be caused by reflectance measurements of a single leaf in those studies versus a canopy measurement made in this study.

The overall conclusion derived from the results presented in Table 2 and Fig. 1 is that remote sensing can be a useful tool to monitor greenbug damage in a wheat crop because statistical differences occurred for all segments of the spectrum (400–900 nm) analyzed. This suggests that broad- and narrow-band imaging sensors can capture surface variations that delineate greenbug damage in field crops, by using an appropriate scale coupled with the infestation size, because image classification methods are based on the similar and dissimilar information contained in an image. Thus, statistical comparisons are made to classify the surface characteristics of an image. Therefore, these results indicate that remotely sensed image could be used to monitor, identify, and discriminate greenbug damage to a wheat crop within a field or across fields in a local area.

Although, as a caveat, using remote sensing for determining greenbug infestation in winter wheat seems to be site specific. Figure 1 shows that the spectral signatures for either infested or uninfested wheat derived from field 1 and field 2 data differ in relative reflectance, indicating that it is not easy, perhaps impossible, to compare fields to one another directly from results presented in this manner. However, if the differences between the spectral signatures for infested and uninfested wheat in the two fields are plotted (Fig. 2), the spectral response was very similar. Plotting the same spectral signature differences for the greenhouse data indicated that there were large differences between the greenhouse and field data. This finding is expected, because greenbug density in the

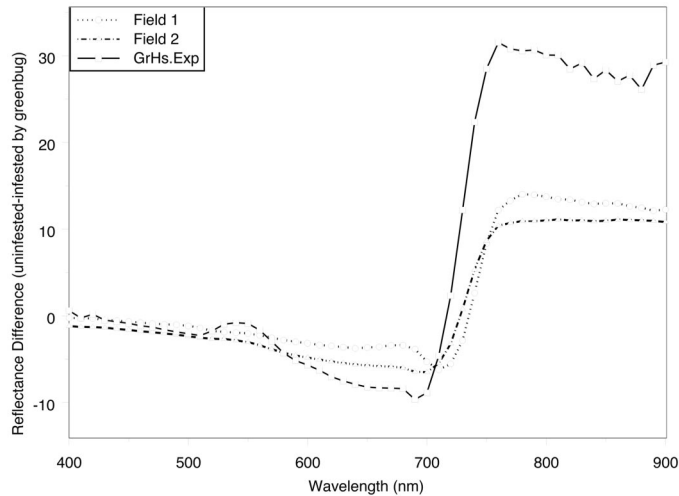


Fig. 2. Percentage of reflectance difference between greenbug-infested and uninfested winter wheat canopies associated with two field and one greenhouse experiment. Field 1, Moore County, near Dumas, TX; $n = 8$. Field 2, Hardeman County near Chillicothe, TX; $n = 18$. GrHs Exp, a greenhouse experiment at the Texas Agricultural Experiment Station facilities at Bushland, TX; $n = 10$.

greenhouse was much higher than in the fields, and there was little to no background noise from exposed soil. Also, the uninfested greenhouse wheat was probably in better condition than the uninfested wheat in the field, not having been exposed to harsh winter conditions, and having relatively clean leaves compared with wheat in the field.

Linear regression analyses confirmed varying relationships between spectral vegetation indices and greenbug density across the fields and greenhouse experiment. The AI had the highest relationships with greenbug density for fields 1 and 2, whereas indices from the literature worked better for the greenhouse experiment compared with AI. This indicates that most of the spectral vegetation indices have the ability to discern robust relationships with high greenbug density, as observed in the greenhouse experiment, but not make the same discernment with lower greenbug densities as found in fields 1 and 2. The relationships between the AI and greenbug densities were more consistent, positive, and significant across the field and greenhouse experiments than the other six indices. Peñuelas et al. (1995) concluded that SIPI minimized the confounding effects of leaf surface and mesophyll structure and was useful for assessment of physiology and phenology of vegetation. Therefore, AI, which was derived from SIPI, seems to be a valid and consistent index to study small grain aphids using remotely sensed data in both field and laboratory conditions.

The poor relationships between the other spectral vegetation indices and greenbug density collected in fields 1 and 2 might be influenced by damage severity. One possible reason for the weaker relationships might be lower damage severity found in fields 1 and 2 compared with the greenhouse experiment (Tables 1 and 3). The mean greenbug damage to wheat was

35% in field 1 and 47% in field 2 (Table 1). Zhang et al. (2003) tested the ability of hyperspectral image data to distinguish the severity of late blight disease from stage 1 (slight) to stage 4 (severe) in tomato. The authors concluded that the diseased vegetation at stages 1 and 2 was difficult to separate from the healthy plants, whereas tomatoes infected by late blight disease at stages 3 to 4 were separated from uninfected tomatoes. Discrimination of healthy rice plants from those lightly infected by rice sheath blight was difficult because of the high overlap in the estimated image indices, whereas identification was more accurate when disease was moderate to severe (Qin and Zhang 2005). Another potential reason for weaker relationships for fields 1 and 2 was the noise added by reflectance of a large soil background. During the data collection, field 2 had the most exposed soil in each of the 18 1-m² plots followed by field 1. The greenhouse experiment results indicated that data collected in a controlled environment produced the strongest correlations among the indices, implying that variation in the greenhouse was much less than that in the field.

The regression results found in this study were strongly supported by the findings of Yang et al. (2005) who identified six wavebands (560, 580, 630, 694, 800, and 830 nm) among the 16 bands of a field radiometer that were more sensitive to greenbug density and damage to wheat because there were larger differences in reflectance values between greenbug-infested and uninfested wheat canopies. Reflectance in these wavebands were strongly correlated (r ranged from 0.68 to 0.96) with greenbug density. This spectral range covers the majority of the wavebands used to calculate vegetation indices given in Table 3 in this study. Yang et al. (2005) reported that vegetation indices might be more sensitive to greenbug infestation because vegetation indices differentiated undam-

aged from damaged wheat at an earlier date in the development of a greenbug infestation than individual wavebands. The correlation coefficients between the NDVI and SR and greenbug density ranged from -0.74 to -0.98 in their study. Yang et al. (2005) and Riedell and Blackmer (1999) discussed the advantage of using vegetation indices over wavebands because vegetation indices have the capacity to reduce the variation in environment due to illumination differences, atmospheric attenuation, cloud and leaf shadowing, and reflectance from the soil, dead material, and litter.

This study showed the usefulness of remotely sensed data to quantify undamaged and damaged wheat due to greenbug feeding at the canopy level in production winter wheat fields. A greenhouse experiment, conducted to verify field data in a controlled condition, was in agreement with the results obtained from two fields. Therefore, hyperspectral remotely sensed data with an appropriate pixel size has the potential to portray greenbug density and discriminate its damage to wheat in production fields with repeated accuracy and precision. In addition, once applied to the image, the relationship between AI and greenbug density and spectral signatures of undamaged and damaged wheat by this aphid will produce density and damage maps. These maps provide detailed spatial and temporal information on greenbug abundance and its damage, which can be used for site specific aphid management in precision agriculture. Future studies should focus on testing image data acquired by satellite or aircraft platforms to detect greenbug or other aphid infestations in small grains at larger scales.

Acknowledgments

Our special thanks to Karl Steddom and Vasilie Catana for help and beneficial discussion. We are thankful to Vanessa Carney, Johnny Bible, Robert Villarreal, David Jones, Timothy Johnson, Steven South, Robert Bowling, Traci Rowland, and Satishreddy Ambati for technical assistance. This study was funded by the USDA-ARS Areawide Pest Management Program, Project 500-44-012-00.

References Cited

- Adams, M. L., W. A. Norvell, W. D. Philpot, and J. H. Peverly. 2000. Spectral detection of micronutrient deficiency in 'Bragg' soybean. *Agron. J.* 92: 261-268.
- Baret, F., and G. Guyot. 1991. Potentials and limits of vegetation indices for LAI and APAR assessment. *Remote Sens. Environ.* 35: 161-173.
- Brooks, H. L. 1991. The greenbug: a pest in wheat. Kansas State University Agricultural Experiment Station and Cooperative Extension Service, MF-925. (<http://www.oznet.ksu.edu/library/entml2/MF925.pdf>).
- Castro, A. M., and C. P. Rumi. 1987. Greenbug damage on the aerial vegetative growth of two barley cultivars. *Environ. Exp. Bot.* 27: 263-271.
- Castro, A. M., C. P. Rumi, and H. O. Arriaga. 1988. Influence of greenbug on root growth of resistant and susceptible barley genotypes. *Environ. Exp. Bot.* 28: 61-72.
- Daughtry, C.S.T., C. L. Walthall, M. S. Kim, E. Brown de Colstoun, and J. E. McMurtrey, III. 2000. Estimating corn leaf chlorophyll concentration from leaf and canopy reflectance. *Remote Sens. Environ.* 74: 229-239.
- Gamon, J. A., and J. S. Surfus. 1999. Assessing leaf pigment content and activity with a reflectometer. *New Phytol.* 143: 105-117.
- Gates, D. M., H. J. Keegan, J. C. Schleiter, and V. R. Weidner. 1965. Spectral properties of plants. *Appl. Optics* 4: 11-20.
- Gilabert, M. A., J. González-Piqueras, F. J. García-Haro, and J. Meliá. 2002. A generalized soil-adjusted vegetation index. *Remote Sens. Environ.* 82: 303-310.
- Gitelson, A. A., and M. N. Merzlyak. 1997. Remote estimation of chlorophyll content in higher plant leaves. *Int. J. Remote Sens.* 18: 2691-2697.
- Gitelson, A. A., M. N. Merzlyak, and O. B. Chivkunova. 2001. Optical properties and nondestructive estimation of anthocyanin content in plant leaves. *J. Photochem. Photobiol.* 74: 38-45.
- Gitelson, A. A., Y. Zur, O. B. Chivkunova, and M. N. Merzlyak. 2002. Assessing carotenoid content in plant leaves with reflectance spectroscopy. *J. Photochem. Photobiol.* 75: 272-281.
- Huete, A. R. 1988. A soil-adjusted vegetation index (SAVI). *Remote. Sens. Environ.* 25: 295-309.
- Jordan, C. F. 1969. Derivation of leaf-area index from the quality of light on the forest floor. *Ecology* 50: 663-666.
- Lamari, L. 2002. ASSESS: Image Analysis Software for Plant Disease Quantification. The American Phytopathological Society Press, St. Paul, MN.
- Lelong, C.C.D., P. C. Pinet, and H. Poilvé. 1998. Hyperspectral imaging and stress mapping in agriculture: a case study on wheat in Beauce (France). *Remote Sens. Environ.* 66: 179-191.
- Malthus, T. J., and A. C. Madeira. 1993. High resolution spectroradiometry: spectral reflectance of field bean leaves infected by *Botrytis fabae*. *Remote Sens. Environ.* 45: 107-116.
- Merton, R. 1998. Monitoring community hysteresis using spectral shift analysis and the red-edge vegetation stress index, pp. 1-14. In *Proceedings of the Seventh Annual PPL Airborne Earth Science Workshop*, 12-16 January 1998, NASA, Jet Propulsion Laboratory, Pasadena, CA.
- Morgham, A. T., P. E. Richardson, R. K. Campbell, J. D. Burd, R. D. Eikenbary, and L. C. Sumner. 1994. Ultrastructural responses of resistant and susceptible wheat to infestation by greenbug biotype E (Homoptera: Aphididae). *Ann. Entomol. Soc. Am.* 87: 908-917.
- Nagaraj, N., J. C. Reese, M. B. Kirkham, K. Kofoid, L. R. Campbell, and T. M. Loughin. 2002a. Effect of greenbug, *Schizaphis graminum* (Rondani) (Homoptera: Aphididae), biotype K on chlorophyll content and photosynthetic rate of tolerant and susceptible sorghum hybrids. *J. Kans. Entomol. Soc.* 75: 299-307.
- Nagaraj, N., J. C. Reese, M. B. Kirkham, K. Kofoid, L. R. Campbell, and T. M. Loughin. 2002b. Relationship between chlorophyll loss and photosynthetic rate in greenbug (Homoptera: Aphididae) damaged sorghum. *J. Kans. Entomol. Soc.* 75: 101-109.
- Nilsson, H. E. 1980. Application of remote sensing methods and image analysis at macroscopic and microscopic levels. University of Minnesota Miscellaneous Publication 7. Agricultural Experiment Station, University of Minnesota, St. Paul, MN.
- Nilsson, H. E. 1991. Hand-held radiometry and IR thermography of plant diseases in field plot experiments. *Int. J. Remote Sens.* 12: 545-557.

- Nilsson, H. E. 1995. Remote sensing and image analysis in plant pathology. *Annu. Rev. Phytopathol.* 15: 489–527.
- Nilsson, H. E., and L. Johnsson. 1996. Hand-held radiometry of barley infected by barley stripe disease in a field experiment. *J. Plant Dis. Prot.* 103: 517–526.
- Peñuelas, J., J. A. Gamon, A. L. Fredeen, J. Merino, and C. B. Field. 1994. Reflectance indices associated with physiological changes in nitrogen- and water-limited sunflower leaves. *Remote Sens. Environ.* 48: 135–146.
- Peñuelas, J., F. Baret, and I. Filella. 1995. Semi-empirical indices to assess carotenoids/chlorophyll *a* ratio from leaf spectral reflectance. *Photosynthetica* 31: 221–230.
- Pinter, P. J., J. L. Hatfield, J. S. Schepers, E. M. Barnes, M. S. Moran, C. S. T. Daughtry, and D. R. Upchurch. 2003. Remote sensing for crop management. *Photogramm. Eng. Remote Sens.* 69: 647–664.
- Qi, J., A. Chenbouni, A. R. Huete, Y. H. Kerr, and S. So-rooshian. 1994. A modified soil adjusted vegetation index. *Remote Sens. Environ.* 48: 119–126.
- Qin, Z., and M. Zhang. 2005. Detection of rice sheath blight for in-season disease management using multispectral remote sensing. *Int. J. Appl. Earth Observ. Geoinf.* 7: 115–128.
- Raikes, C., and L. L. Burpee. 1998. Use of multispectral radiometry for assessment of *Rhizoctonia* blight in creeping bentgrass. *Phytopathology* 88: 446–449.
- Richardson, A. D., M. Aikens, G. P. Berlyn, and P. Marshall. 2004. Drought stress and paper birch (*Betula papyrifera*) seedlings: effects of an organic biostimulant on plant health and stress tolerance, and detection of stress effects with instrument-based, noninvasive methods. *J. Arboricult.* 30: 52–61.
- Riedell, W. E., and T. M. Blackmer. 1999. Leaf reflectance spectra of cereal aphid-damaged wheat. *Crop Sci.* 39: 1835–1840.
- Rondeaux, G., M. Steven, and F. Baret. 1996. Optimization of soil-adjusted vegetation indices. *Remote Sens. Environ.* 55: 95–107.
- Rouse, J. W., R. H. Naas, J. A. Schell, and D. W. Deering. 1973. Monitoring vegetation systems in the Great Plains with ERTS, pp. 309–317. *In* Third ERST Symposium, NASA Sp-351, vol. 1, Washington, DC.
- Tucker, C. J. 1979. Red and photographic infrared linear combinations for monitoring vegetation. *Remote Sens. Environ.* 8: 127–150.
- Yang, Z., M. N. Rao, N. C. Elliott, S. D. Kindler, and T. W. Popham. 2005. Using ground-based multispectral radiometry to detect stress in wheat caused by greenbug (Homoptera: Aphididae) infestation. *Comp. Electr. Agric.* 47: 121–135.
- Zadok, J. C., T. T. Chang, and C. F. Konzak. 1974. A decimal code for the grown stages of cereals. *Weed Res.* 14: 415–421.
- Zhang, M., Z. Qin, X. Liu, and S. L. Ustin. 2003. Detection of stress in tomatoes induced by late blight disease in California, USA, using hyperspectral remote sensing. *Int. J. Appl. Earth Observ. Geoinf.* 4: 295–310.

Received 1 September 2005; accepted 26 June 2006.